Arch Neurosci. 2015 January; 2(1): e19257. DOI: 10.5812/archneurosci.19257

Published online 2015 January 1. **Research Article**

Separating Mental Disorders Using Vestibular Field Potentials

Jerome Joseph Maller [1]; Monash Alfred [2,3,4]; Caroline Gurvich [1]; Saman Haghgooie [3]; Omid Ranjbar Pouya [5]; Paul Bernard Fitzgerald [1]; Jayashri Kulkarni [1,*]

[1]Monash Alfred Psychiatry Research Centre, The Alfred Hospital, Monash University Central Clinical School, Melbourne, Australia
[2]Psychiatry Research Centre, The Alfred Hospital, Monash University Central Clinical School, Melbourne, Australia
[3]Diagnostic and Neurosignal Processing Research Group, Department of Electronic Engineering and Computing Science, Monash University, Clayton, Melbourne, Australia
[4]Department of Electrical and Computer Engineering, University of Manitoba, Winnipeg, Canada
[5]Biomedical Engineer, Department of Electrical and Computer Engineering, University of Manitoba, Winnipeg, Canada

*Corresponding author: Jayashri Kulkarni, Monash Alfred Psychiatry Research Centre, The Alfred Hospital and Monash University Central Clinical School, Melbourne, Australia. Tel: +61-390766564, Fax: +61-390766588 Email:, E-mail: j.kulkarni@alfred.org.au

Received: March 9, 2014; **Revised:** March 28, 2014; **Accepted:** March 30, 2014

Background: Absence of quantitative techniques for objectively diagnosing many brain changes associated with mental illnesses hampers early intervention and effective treatment. Known bidirectional neural pathways closely link the vestibular system and regions involved in emotion processing.
Objectives: To assess whether Electrovestibulography (EVestG) can detect specific neural responses, using an ear probe and tilt chair, to provide a quantitative indirect measure assessment of brain regions and pathways frequently compromised in mental illnesses.
Materials and Methods: EVestG data was collected on 38 subjects with major depression, 22 with schizophrenia, 36 with bipolar disorder and 57 matched healthy controls. Data was analyzed using the NEER algorithm to generate the average field potentials and firing patterns. Characteristic features were extracted followed by AdaBoost subset feature selection and classification for separating data into four classes. To remove the bias of working on small size population, we used 10-fold cross validation to select the best diagnostic features. The accuracy of the diagnostic features' classification was tested using nonparametric statistical analysis.
Results: EVestG signals were statistically different (P = 0.000 to 0.040) between the groups by using Kruskal-Wallis, and the best diagnostic accuracies for a four-way diagnostic group separation were on average (n = 100, 10 repeated 10-fold cross validations) 70.2% (SD = 9.6) using 10-fold cross validation.
Conclusions: Comparing vestibular driven responses has the potential to be a valid and clinically useful diagnostic tool.

Keywords: Depression; Schizophrenia; Bipolar Disorder

1. Background

According to the World Mental Health (WHO) Survey Consortium, the worldwide prevalence of mental illness is high, with a significant percentage of individuals developing one or more mental illnesses in their lifetime (1). Mental illnesses have profound personal, social and economic costs that are often underestimated. Despite tremendous efforts in recent years, there are currently no objective and quantitative techniques to inexpensively, accurately and rapidly diagnose common mental illnesses. Emergence of testing systems that can identify early illness and monitor disease progression and treatment response would represent a significant advance to promote early intervention and fast tracking of new treatments for mental illnesses (2). Recent research suggests that the vestibular system is a potential window for exploring psychiatric conditions. For a review see Gurvich study (3). Specifically, the parabrachial nucleus (PBN) network provides a direct link between the vestibular system and neural networks involved in emotional processing. For example, the PBN has reciprocal connections with the vestibular nuclei (4-6), as well as reciprocal connections with the amygdala, hypothalamus, locus coeruleus (which also has bidirectional links to the vestibular nuclei and emotion areas), and prefrontal cortex (4, 7, 8). The amygdala, hypothalamus, locus coeruleus and prefrontal cortex are all areas commonly linked with mental illnesses such as schizophrenia (SCZ), bipolar disorder (BPD), major depressive disorder (MDD) (9-11). Importantly, there are direct associations between the vestibular system and the hippocampus, a brain region consistently implicated in models of psychiatric disorders. For example, vestibular stimulation increases neuronal firing in the hippocampus, and studies have demonstrated that spatial navigation is influenced by the vestibular-hippocampus connectivity (12-15). Furthermore, it has been shown that there is a direct association between vestibular stimulation and mood changes (16). Recently, we have introduced a novel diagnostic technique named electrovestibulography (EVestG). We hypothesize that this method can detect specific vestibuloacoustic and more particularly vestibular field potentials, subsequently providing a quantitative and indirect measure of activity in brain regions and neural pathways that are frequently compromised in neuropsy-

chiatric diseases. In this paper, we present preliminary evidence that these signals have potential to be developed as useful diagnostic tools to diagnose mental illnesses.

1.1. Measuring the Vestibular Response

EVestG is a recently developed technique designed to detect specific vestibuloacoustic and more particularly vestibular field potentials (17), subsequently providing a quantitative and indirect measure of activity in brain regions and neural pathways that are frequently compromised in neuropsychiatric diseases. EVestG measures a vestibular driven response stimulated by whole body passive tilts using a computer-controlled hydraulic tilt chair with a sinusoidal velocity profile (17). The recording is based on one tilt applied to each plane. The chair is designed to roll with angular motions (Figure 1 a), to pitch and perform smooth sinusoidal yaw and translational up-down motion.

Figure 1. Electrovestibulography System

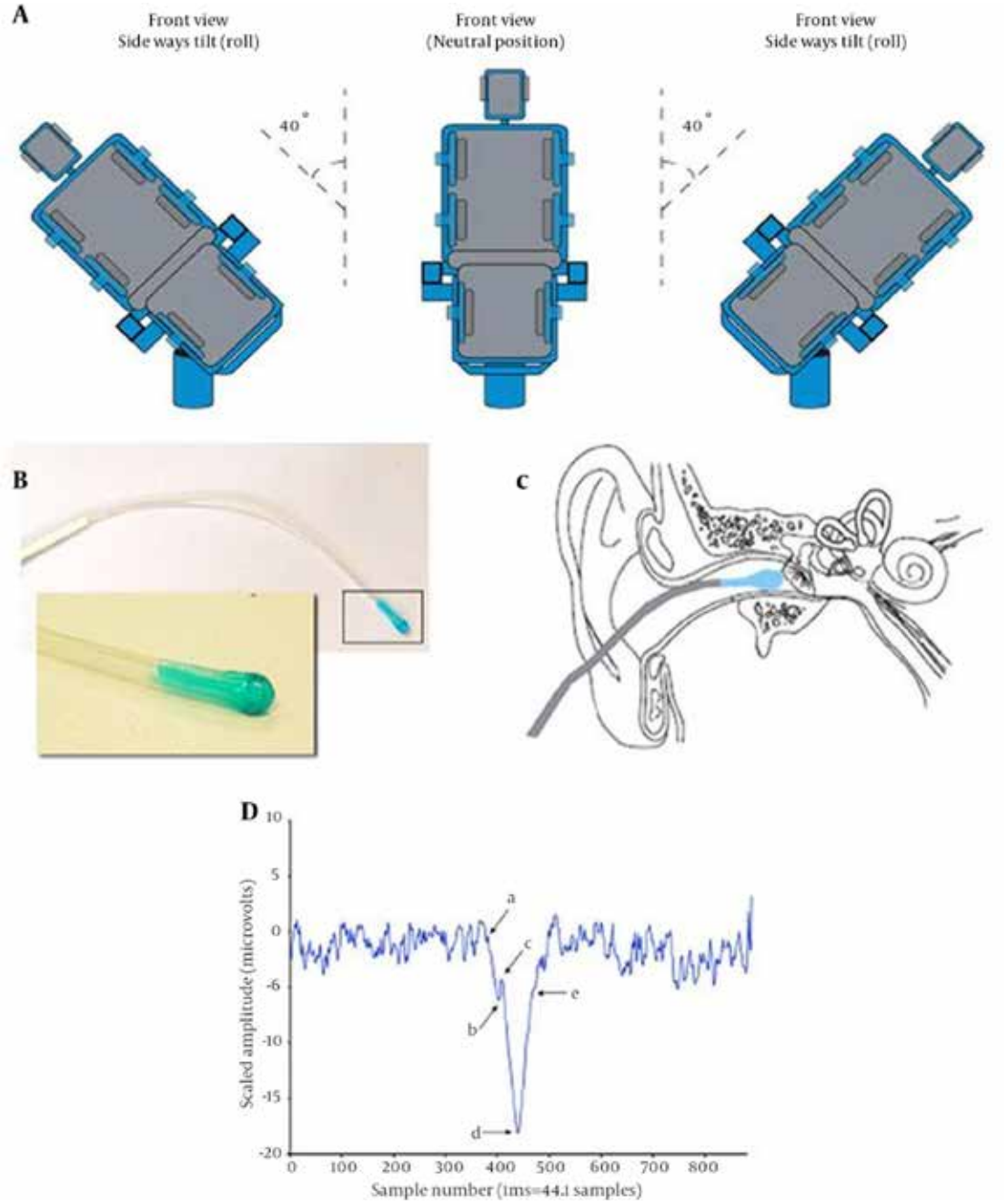

A, Angles used for the sideways tilt; B, The electrode used for electrovestibulography; C, Diagram of the placement of the electrode in the ear; D, Output of the Neural Event Extraction Routine (NEER) algorithm, where (a) indicates the baseline or Summating Potential (SP) start point, (b) indicates the SP notch, (c) indicates the beginning of Action Potential (AP) top, d indicates AP, and (e) indicates AP rise.

The signal was obtained via a gelled electrode consisting of a wick (Figure 1B) positioned to rest close to the tympanic membrane (but not touching it) (Figure 1C). Recordings were taken during the dynamic and static phases (i.e. when the tilt chair is moving and stationary) and during excitatory and inhibitory responses (e.g. rotational motion provides an excitatory effect on the horizontal semicircular canal for rotations that are ipsilateral toward the motion direction and an inhibitory effect for contralateral tilts). A wavelet-based signal processing technique called the Neural Event Extraction Routine (NEER, 18) was used to detect the spontaneous field potentials and their firing patterns from the noise floor in the recorded signals. The NEER algorithm averages the detected field potentials to produce a Summing Potential/Action Potential (SP/AP) plot and the firing pattern of the field potentials occurrence like those shown in Figures 3 and 4. The key advantages of EVestG over other measures of vestibular function (i.e., vestibular ocular reflex) are that it detects a direct rather than indirect vestibular response, hypothesized to be driven particularly from the utricle (18). The use of whole body tilts minimizes neck muscle artifacts and other head movement-induced neural signals.

2. Objectives

The aim of the current study was to investigate the potential capacity of features extracted from EVestG to distinguish key psychiatric diagnostic groups and healthy controls. We hypothesize that the differences between the psychiatric and control groups would be significant.

3. Materials and Methods

3.1. Participants

People with one of the three following common mental illnesses were recruited and assessed: major depressive disorder (MDD), bipolar disorder (BPD) and schizophrenia (SCZ). All participants should have one illness only; hence, those who had a history or current symptoms of an additional psychiatric or neurological condition were excluded. We also recruited a number of healthy age and gender matched control subjects who were examined after undergoing exclusion tests for psychiatric illnesses. The study was approved by The Alfred Human Ethics Committee (Approval Number 95/06) and all subjects signed an informed written consent prior to the experiments.

3.1.1. Clinical Characteristics

3.1.1.1. Major Depressive Disorder (MDD)

Thirty-eight individuals (13 males) with a DSM-IV diagnosis of MDD were included (Mean age of 46.3 ± 11.9 years). A psychiatrist confirmed the diagnosis. The depression experienced at the time of testing was quantified using the Montgomery-Asberg Depression Rating Scale (MADRS) (19). The mean depression score was 18.54 (SD = 9.4) and the average disease duration was 16.5 years (SD = 9.4). These scores suggested that this was a group with moderate to severe depression. Twenty-three of the MDD participants were taking antidepressant medications including Selective Serotonin Re-uptake Inhibitors (SSRIs) and Serotonin and Noradrenergic Re-uptake Inhibitors (SNRIs), while the rest fifteen patients were not taking any antidepressant medications. Twenty-six of the MDD participants with depression had a family history of depression.

3.1.1.2. Schizophrenia (SCZ)

Twenty-two individuals (14 males) with a DSM-IV diagnosis of SCZ were included (mean age = 43.0 years, SD = 9.1). A psychiatrist confirmed the diagnosis. Symptoms of psychosis were quantified using the Positive and Negative Syndrome Scale (PANSS) (20). The mean score was 64.4 (SD = 13.2) and the average disease duration was 12.0 years (SD = 8.3). Hence, this group had established, moderately severe SCZ. Two participants were not taking any medications, 19 were taking a newer type of antipsychotic and one was taking an older injectable antipsychotic. Thirteen of the participants with SCZ had a family history of SCZ.

3.1.1.3. Bipolar disorder (BPD)

Thirty-six patients (19 males, 49.0±14.1 years) with a DSM-IV diagnosis of BPD were tested. Psychiatrists (JK and PF) confirmed the diagnosis. The mean age of BPD group was 49 years (SD = 14.1) and the illness duration was 15.7 years (SD = 11.3). Eleven patients had type I, 11 had type II and in 14, the type was unknown. We quantified the depression and mania symptoms experienced by the participants using the MADRS rating scale for depression, and the Young Mania Rating Scale (YMRS, (21)). The mean MADRS score was 13.7 (SD = 10.7), and the mean YMRS was nine.5 (SD = 7.5). This suggests that the group had longstanding illness and most patients experienced depression as a part of their illness rather than mania at the time of testing. One patient was taking no medication and the rest were taking combinations of mood stabilizers (lithium, sodium valproate and carbamazepine) and/or newer antipsychotics and/or antidepressant medications. Thirty people in this group had a family history of BPD.

3.1.1.4. Healthy Controls

Fifty-seven (20 males, 34.5 ± 14.8 years) without a history of a psychiatric disorder were included as a healthy control group (mean age = 34.5 years, SD = 14.84). These participants were screened for psychiatric illness and cognitive decline with the Mini-International Neuropsychiatric Interview (M.I.N.I.) screening tool, the Mini Mental State Examination (MMSE) (mean = 29.6, SD = 0.8) and MADRS (mean = 3.1, SD = 4.3)

3.2. Testing Procedures

Each participant seated upright in a hydraulically operated tilt chair, placed inside an electromagnetically shielded and sound attenuated (> 30 dB) chamber. Assessments were conducted with participants' eyes closed, in a relaxed state with their neck supported. Recordings were taken before, during and after each chair tilt. The degree of movement of the chair extended to 40 degrees of yaw, pitch and roll movement and 15 cm of vertical translation. The vertical translation (up-down movement)and yaw recording could also be performed with the subject in the supine position. To acquire the recording, an active pregelled electrode was placed noninvasively in each ear canal proximal to the tympanic membrane, without discomfort to the subject. Reference electrodes were placed on the ipsilateral earlobes and a common ground electrode placed on the forehead. Figure 1 shows the schematic view of the experiment. A practice recording/tilt was made before each recording to familiarize the subjects with the procedure, completed in less than 30 minutes. The subject remained passive throughout the test, and was not required to interact cognitively during the measurement.

3.3. Analysis of the Electrovestibulography Recordings

The NEER algorithm (17) was used to generate the average field potential response and its firing pattern from each time segment of the recorded signal during the chair tilt. For details of signal processing techniques used in the NEER algorithm please see the recent publication (17). Signals were examined for muscle corruption and consequential saturation. If the signal corruption lasted for more than 50% of the signal phase or there was a significant power line or hydraulic artifact, it was rejected and omitted from the analysis. Several features, or biomarkers, such as amplitude, latency and baseline shifts, as well as change in the firing pattern (which is representative of neural synchronization and depicted as an interval histogram change) in moving from a static to dynamic phase were extracted from the average field potential and the firing pattern histogram as the two output signals of NEER algorithm. Either alone or combined, these features were analyzed to identify and statistically differentiate responses of healthy participants and different psychiatric patients. Each signal includes two main tilting responses, a resting (BGi) and an acceleration (onAA) or deceleration (onBB) phase response; in addition, we recorded from both left and right ears. Therefore, extractable features are numerous; however, the number of significant features statistically exceeds random obtainable features. Therefore, at first stage of the study, we ran a simple statistical test to select features that were the most statistically different pairwise between each patient group and controls; 36 features were selected at this stage (see Table 1). Then, we used AdaBoost (22) feature selection and classification which incorporated 10-fold cross validation (see below) to select the features that can best classify the entire population into 4 groups. To assist the selection of features, all 36 features were tested with an Independent-Samples Median Test to ensure good separability ($P < 0.05$).

Any classification technique needs some data for training. In a large dataset, training set is normally selected as a random selection of 50% of the population. However, this cannot be performed in small datasets such as the one in this study. In case of small population, the common solution is to use leave-10-out (10 fold cross validation 10FCV) routine to have an enough training dataset and avoid the over fitting and bias problem (23, 24). In this routine, 10% of the data is set aside randomly as testing, and classification algorithm is trained using the rest of data and tested on the 10% left-out dataset. This routine is repeated 10 times until all the subsets are used as test once, and the overall accuracy would be the average accuracy at each trial. Hence, it attempts to use limited data without its inclusion in any training or feature selection algorithm. Figure 2 illustrates the flowchart of data processing. The following subsections describe the features and classifications in more detail.

Table 1. Feature Data[a,b]

Feature Number and Group	Feature Type	Motion Direction	Motion Phase	Side	Description	Independent-Samples Median; Test (P Value)	Bonferroni-Dunn Ad Hoc; Groups with Significant Difference (Q Statistic)	Feature Value; (Pairwise, Greedy)	
SCZ vs. CTL									
1	FP	ipsilateral roll	S-D acceleration	L	prePP	0.002	MDD-SCZ(4.33), MDD-BPD(2.73), CTL-SCZ(2.79)	0.35	0.30
2	FP	vertical translation	RTC deceleration	L	PostPP to AP	0.033	CTL-SCZ(3.08)	0.32	0.35
3	IH	backward pitch	BGi minus RTC BGi	L	bin 17	0.004	CTL-SCZ(3.72), MDD-SCZ(3.01)	0.27	0.36
4	IH	ipsilateral roll	BGi minus RTC BGi	L	bin 11	0.013	CTL-SCZ(3.40)	0.35	0.39
5	TAP	ipsilateral roll	acceleration	L	baseline	0.082	-	0.39	0.32
6	TAP	prone vertical translation	BGi minus RTC BGi	R	Nah	0.052	-	0.43	0.48
SCZ vs. BPD									

7	FP	vertical translation	deceleration	R	PostPP	0.261	-	0.37	0.32
8	FP	backward pitch	acceleration	R	prePP to AP	0.232	-	0.31	0.38
9	IH	contralateral roll	S-D RTC deceleration	L	bin 15	0.011	BPD-SCZ(3.33)	0.18	0.30
10	IH	prone vertical translation	S-D acceleration	R	bin 11	0.127	-	0.29	0.38
11	TAP	contralateral roll	S-D RTC acceleration	R	Naz	0.078	BPD-SCZ(2.72), MDD-SCZ(2.70)	0.32	0.29
12	TAP	backward pitch	S-D acceleration	L	Nah	0.004	BPD-SCZ(3.04)	0.38	0.36
SCZ vs. MDD									
13	FP	contralateral roll	RTC deceleration	L	PostPP	0.001	MDD-SCZ(2.73), MDD-CTL(2.99), MDD-BPD(2.74)	0.33	0.34
14	FP	vertical translation	BGi minus RTC BGi	R	PostPP to AP	0.123	BPD-SCZ(3.04)	0.27	0.32
15	IH	vertical translation	S-D RTC acceleration	R	bin 9	0.04	MDD-SCZ(2.69)	0.27	0.35
16	IH	contralateral roll	S-D acceleration	L	bin 8	0.29	MDD-SCZ(2.76)	0.31	0.36
17	TAP	contralateral roll	S-D RTC acceleration	R	TAPh	0.322	-	0.31	0.33
18	TAP	backward pitch	BGi minus RTC BGi	L	Nah	0.096	BPD-SCZ(2.72)	0.37	0.36
MDD vs. CTL									
19	FP	backward pitch	S-D sum all phases	L	PostPP to AP	0.059	MDD-CTL(3.0)	0.33	0.38
20	IH	ipsilateral roll	S-D acceleration	R	bin 12	0.014	MDD-CTL(3.12)	0.28	0.43
21	IH	ipsilateral roll	S-D RTC deceleration	L	HF-LF	0.003	MDD-CTL(3.52)	0.28	0.36
22	IH	yaw	S-D deceleration	L	bin 12	0.004	MDD-CTL(3.78)	0.34	0.37
23	TAP	contralateral roll	S-D deceleration	L	Kh	0.016	MDD-CTL(2.97), MDD-BPD(3.47)	0.25	0.34
24	TAP	vertical translation	deceleration	L	Kh	0.027	MDD-CTL(3.09)	0.40	0.42
BPD vs. CTL									
25	FP	vertical translation	BGi minus RTC BGi	L	PrePP to AP	0	BPD-CTL(6.67), MDD-CTL(5.09), CTL-SCZ(3.71)	0.49	0.45
26	FP	contralateral roll	S-D acceleration	L	PostPP	0.169	-	0.38	0.48
27	IH	yaw	BGi minus RTC BGi	L	bin 15	0.2	CTL-SCZ(3.38), BPD-CTL(3.50), MDD-CTL(2.79)	0.30	0.31
28	IH	prone vertical translation	BGi minus RTC BGi	L	bin 6	0.001	CTL-SCZ(2.87), BPD-CTL(3.60), MDD-CTL(3.55)	0.34	0.40
29	TAP	ipsilateral roll	BGi	R	TAPh	0.086	-	0.36	0.38
30	TAP	ipsilateral roll	RTC acceleration	L	TAPh	0.083	MDD-BPD(2.73), BPD-CTL(2.91)	0.36	0.40
MDD vs. BPD									
31	FP	backward pitch	acceleration	R	PrePP to AP	0.232	-	0.32	0.39
32	FP	contralateral roll	acceleration	L	PostPP to AP	0.006	MDD-BPD(2.98)	0.22	0.35
33	IH	contralateral roll	S-D RTC deceleration	R	bin 20	0.226	MDD-BPD(2.84)	0.43	0.41
34	IH	prone vertical translation	S-D RTC acceleration	R	bin 5	0.299	-	0.29	0.38
35	TAP	contralateral roll	S-D acceleration	L	Kh	0.012	MDD-BPD(3.03)	0.28	0.33
36	TAP	ipsilateral roll	RTC acceleration	L	Kh	0.213	MDD-BPD(3.07), BPD-CTL(3.03)	0.33	0.36

[a] Abbreviations: FP, field potential shape feature; IH, interval histogram bin feature; TAP, field potential time feature; Bin, specific time interval range between subsequent field Potentials; RTC, return to center from displaced position

[b] Each feature was selected primarily based on the AdaBoost feature value within each feature group. This was selected if the Independent- Samples Median Test P value was < 0.05 else the next lowest AdaBoost value in each feature group. BGi is the 1.5 seconds of recording immediately prior to movement. S-D is Static minus Dynamic e.g. BGi-onAA. Critical Q statistic 2.6310

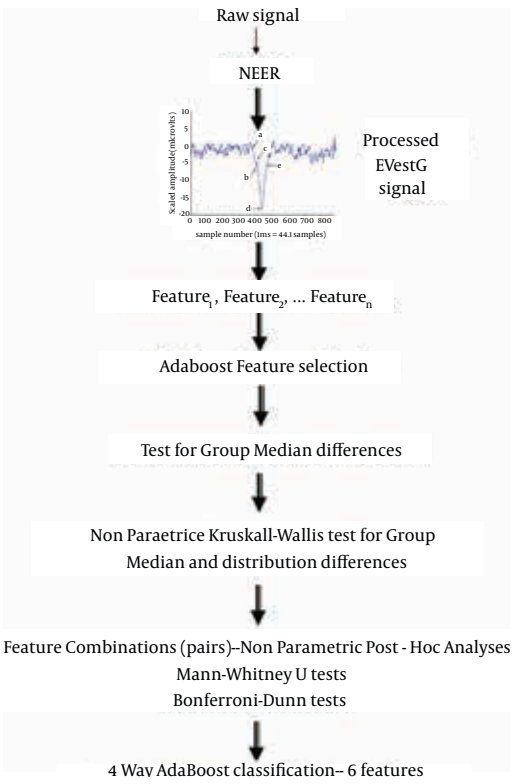

Figure 2. Schematic Flowchart of the Data Processing

Figure 3. Potential/Action Potential (SP/AP) Plot and the Firing Pattern of the Field Potentials

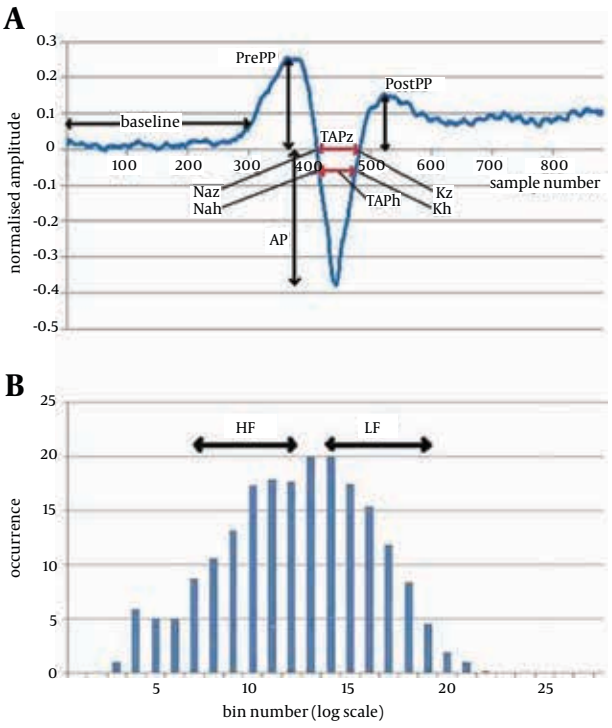

3A. A typical detected average field potential.Ap point: The minimum value in the range of 437-448 samples; Sp point: A notch found 15-30 samples before the Ap point; PrePP: Maximum value in the range of 293-389 samples; PostPP: Maximum value in the range of 498-548 samples; Baseline: The average value in the range of 50-250 samples; TAPz: The distance between the two points where the FP curve crosses the baseline; TAPh: The distance between the two points where the FP curve crosses the line half way between the PrePP and AP. These features are measured in the static and dynamic phases and difference used as the analysed feature.3B. Normalised Histogram of the firing pattern. The difference between consecutive time of detected field potentials plotted using 25 bins logarithmically spread (0.5-50 msec). Can be grouped into Low Int: The sum of the values of the histogram in bins 7-12 and High Int: The sum of the values of the histogram in bins14-19. These features are measured in the static and dynamic phases and difference used as the analysed feature.

3.3.1. Feature Selection

Most of the features selected from averaged field potential shape and the firing interval pattern reflect the changes in response pattern when moving from a stationary to a dynamic phase (to a static phase), and were based on the smallest p value measured for discriminability between pairs of groups. Figures 3 and 4 show the two main signals and some of the extracted features.

Thirty-six significant features selected at stage 1 of the analysis (Table 1), were selected statistically for each pairwise separation of each two groups of the data (e.g. BPD and MDD). These features were not necessarily normally distributed; thus, nonparametric analysis was required. These 36 features were input to a 4-group AdaBoost (22) feature ranking system (Table 1, second last column). Two selection methods were used. Method 1: Initially six of the 36 features were selected for detailed analysis, to examine separability, and to provide the best separation and classification accuracy for the 4 group separation using a limited number of features (Table 1, Rows highlighted). One feature was selected from each feature Group. Each feature was selected primarily based on the AdaBoost pair-wise feature value within each feature group. This feature was selected if the Independent- Samples Median Test p value was < 0.05 (Table 1, column 8) otherwise the next lowest AdaBoost pair-wise value in each feature group was used and so on. Method 2: An AdaBoost "greedy" algorithm (after the first feature, selection of subsequent features is dependent on the selection of previous features to minimize the feature commonality) was applied. Based on the AdaBoost feature selection value (last column Table 1), the best combination of features was sought to achieve the best accuracy and >70% with the minimum number of features.

Kruskal-Wallis nonparametric statistical analysis (the equivalent of a 1 way ANOVA for nonparametric data) was undertaken on the selected six features using SPSS (Ver. 19; SPSS Inc, Chicago, Illinois) to investigate the statistical difference between the groups. These pairwise comparisons provide p-values for group median and distribution differences. Analyses were two-tailed at a significance level of P = 0.05. Furthermore, the selected features were input to a Bonferroni-Dunn analysis (25) using Matlab Version 2010b (fx = dunn.m, (26)) and Mann-Whitney

U test (using SPSS) was used to provide nonparametric post-hoc analysis (the equivalent of the Bonferroni correction) and to test for significant differences between the groups. Some of the select features exhibited more than one significant pair-wise separation.

4. Results

4.1. Vestibular Testing Results

The six selected features (Method 1) provided a separation and classification accuracy for the four groups separation of 60.1% (SD = 11.7). An analysis of median group values (Figure 4) graphically summarizes the feature trends and shows for:

- Feature 1 significant differences between the all groups except BPD and CTL
- Feature 12 significant differences between the all groups except MDD and CTL
- Feature 13 significant differences between SCZ and MDD/BPD groups
- Feature 24 significant differences between MDD in the all groups
- Feature 25 significant differences between CTL and BPD/MDD/SCZ
- Feature 35 no significant differences but the largest between BPD and SCZ/MDD

The TAP features (field potential time axis features) provided some good separations but at a reduced significance compared to the field potential shape and firing pattern features used. The Kruskal-Wallis analyses also showed significant differences between the all groups for the six selected features, and mostly at the level of $P \leq 0.011$ (significance for Feature 1 = 0.000; Feature 12 = 0.019; Feature 13 = 0.007; Feature 24 = 0.003; Feature 25 = 0.000; Feature 35 = 0.015). More significantly, Tables 2 and 3 show the comparison of the selected EVestG features between the healthy control participants and those with BPD, MDD and SCZ, demonstrating significant separation between the groups. Bonferroni-Dunn (Table 1) and Mann-Whitney U results (Table 2) demonstrated that each feature has 1-3 significant differences between the pairs of groups. An AdaBoost pair-wise 4 pathology classification was applied using the six features examined above as a set. 10FCV was applied to the analysis. The result had a 60.1% accurate classification on average (95% confidence range was 52-68%, SD = 11.7% using n=100, 10 repeated 10 fold cross validations). Finally, an AdaBoost "greedy" feature selected group of features was input to an AdaBoost classifier for a 4-pathology classification. A classification accuracy of 70.2% (95% confidence range was 63-77%, SD = 9.6% using n = 100, 10 repeated 10 fold cross validations) was achieved using 13 features [1, 5, 6, 10, 15, 23, 25, 26, 27, 28, 30, 32, 34]. Increasing the number of features beyond 13 produced on marginal improvements in accuracy (Table 3).

Figure 4. EVestG Group Median for Each Feature

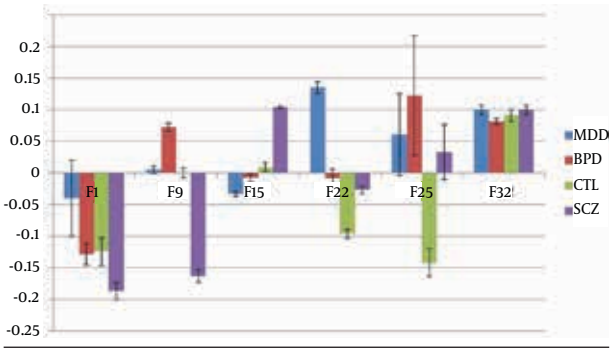

Error bars represent variance. Vertical axis is nominal to best display 6 features on same axes.

Table 2. Mann-Whitney U Test Between Groups in Pair[a,b]

Groups	Feature 1	Feature 12	Feature 13	Feature 24	Feature 25	Feature 35
MDD vs. BPD						
Z	-2.923	-1.586	-2.793	-0.661	-1.654	-3.078
P value	0.003	0.113	0.005	0.509	0.098	0.002
MDD vs. CTL						
Z	-2.406	-0.670	-2.921	-2.979	-5.073	-2.520
P value	0.016	0.503	0.003	0.003	0.001	0.012
MDD vs. SCZ						
Z	-3.59	-1.771	-2.764	-2.726	-0.811	-1.099
P value	0.001	0.077	0.006	0.006	0.417	0.271
BPD vs. CTL						
Z	-0.929	-1.787	-0.034	-2.506	-6.21	-0.738
P value	0.353	0.074	0.973	0.012	0.001	0.461
BPD vs. SCZ						
Z	-2.568	-3.554	-0.436	-2.062	-2.298	-1.364
P value	0.01	0.001	0.663	0.039	0.022	0.173
CTL vs. SCZ						
Z	-2.887	-1.175	-0.361	-0.186	-4.375	-0.817
P value	0.004	0.240	0.718	0.852	0.001	0.414

[a] Abbreviations: SCZ, schizophrenia, BPD, bipolar disorder, MDD, major depressive disorder.
[b] Z, Z score; P, significance level (2-tailed); bolded data represent significant differences ($P \leq 0.05$). Results are shown for the six best selected features.

Table 3. AdaBoost Classifier Accuracies Using AdaBoost "Greedy" Feature Selection[a]

Feature Set	Accuracy	SD
26	48.04	-
26, 25	55.42	7.27
26, 25, 23	57.37	8.80
26, 25, 23, 34	59.17	9.81
26, 25, 23, 34, 32	61.12	10.47
26, 25, 23, 34, 32, 15	63.00	9.01
26, 25, 23, 34, 32, 15, 28	61.83	8.57
26, 25, 23, 34, 32, 15, 28, 6	60.54	9.62
26, 25, 23, 34, 32, 15, 28, 6, 1	64.42	6.23
26, 25, 23, 34, 32, 15, 28, 6, 1, 10	68.92	10.54
26, 25, 23, 34, 32, 15, 28, 6, 1, 10, 5	68.21	9.57
26, 25, 23, 34, 32, 15, 28, 6, 1, 10, 5, 27	68.21	8.10
26, 25, 23, 34, 32, 15, 28, 6, 1, 10, 5, 27, 30	70.17	9.56
26, 25, 23, 34, 32, 15, 28, 6, 1, 10, 5, 27, 30, 36	70.21	11.38
26, 25, 23, 34, 32, 15, 28, 6, 1, 10, 5, 27, 30, 36, 19	69.58	12.91

[a] Date are presented as %

5. Discussion

The results presented here expand upon our previous work (17) using electrovestibulography (EVestG) as a novel diagnostic technique, which can noninvasively detect and record vestibulo-acoustic potentials, predominantly vestibular-driven field ones. In the current study, the resulting features demonstrated good specificity and sensitivity to diagnose several key psychiatric illnesses in a difficult 4-way classification problem. Differentiating between psychiatric conditions is a major challenge. As an initial step towards clarifying diagnoses, we were interested in whether features, as measured by EVestG, it is possible to differentiate various mental illnesses. This capacity to separate different psychiatric diagnostic groups is demonstrated (Figure 4). The fact that the results were based on a 10-fold cross validation, ensures the robustness of the results and removes the bias and over fitting problems of the small sample size. These robust results are very encouraging, particularly when differentiating difficult diagnoses such as BPD and MDD. Basco (27) reported that in one-half of their cases studied, there was disagreement between the DSM-III and the routine clinical diagnosis. However, the stringent application of DSM-III structured clinical interviews [SCID] together with a detailed medical history over a three-hour interview led to 90% diagnostic sensitivity and specificity. The model of pathways involved in psychiatric and vestibular symptoms in detailed in our previous publication (3). EVestG features may be mediated by disruptions in emotion processing centers, involving the parabrachial nucleus and locus coeruleus, linked with central or even peripheral parts of the vestibular system. The use of a 10-fold cross validation technique indicated that all clinical separations remained coherent with diagnostic values close to 70%, suggesting that the EVestG technique is potentially a valid and clinically useful diagnostic tool.

Vestibular stimulation in humans has been shown to induce activity in three brain regions of hippocampus (HC), retrosplenial cortex, and parietal lobe (14, 20-28). These are among regions consistently reported to have abnormal findings in MDD and SCZ when compared to healthy controls (14, 28-38). See (3) for a review. Some studies reported that these regions had reduced gray and/or white matter volumes (34, 39), and/or altered blood flow (35-37)

There are known associations between the vestibular system and the HC, particularly the dorsal (posterior) segment (40). It has been shown in both small animals and humans that vestibular stimulation directly activates head direction and place cells within the dorsal HC (41-43). Not surprisingly, it has also been demonstrated that vestibular compromise directly relates to reduced spatial memory and navigation (12, 13, 41) and cognitive skills have been shown to be related to the dorsal HC (44-46) specifically place cells (41). Comorbidity between vestibular and psychiatric disorders is underestimated, untreated, and may result in a chronic status and poor quality of life (47). The dorsal HC is a vulnerable region in the context of psychiatric disorders, specifically depression and SCZ, and particularly in those who are treatment-resistant (34), i.e. their symptoms do not respond appreciably within a given time across at least three types of medications. The dorsal HC is rich in serotonin receptors, and a major target of antidepressants, so a smaller dorsal HC provides fewer (if any) targets for the medication to act on. By contrast, the anterior thalamus has been implicated in vestibular-HC models (48); damage to this region does not alter the vestibular-HC relationship for vestibular stimulation and increased cell firing in the HC, retrosplenial region, or parietal lobe (49, 50). However, it is not implicated in models of depression or SCZ. The features extracted from the average field potentials and their interval-firing pattern (the outputs of the NEER algorithm) statistically separate the groups from each other. Our hypothesis is that EVestG is an index of the integrity of brain regions related to psychiatric disorders. If one of those regions is damaged (e.g. HC), the EVestG signal would be different with people with no damaged HC (e.g. /i.e. healthy controls with no history of psychiatric disorders). Our group showed that the HC volume significantly reduced in patients with MDD compared with healthy controls, specifically in the dorsal region, but this reduction was even greater in those with SCZ (34). Our results indicated a greater statistical difference between SCZ and healthy controls than between MDD and healthy controls, which is consistent with our hypothesis. As a further example, we found that white matter integrity is reduced only in the parietal lobe (one of the three regions reported to be directly related to vestibular stimulation) in those who developed MDD after experiencing a mild traumatic brain injury (51).

Projecting from the hippocampus, retrosplenial cortex (Brodmann Areas of 26, 29 and 30) is considered a part of the posterior cingulate gyrus, a region central to mem-

ory performance, which is compromised in psychiatric disorders, such as MDD, BPD and SCZ (52). More specifically, the cingulate and retrosplenial regions are major components of the dorsomedial limbic cortex (53). The cingulate gyrus extends anteriorly into the prefrontal regions and then inferiorly into the orbitofrontal region, and is also a major intersection for frontal lobe connectivity and implicated in conventional models of psychiatric disorders (54, 55). It is interesting to look at 36 features listed in Table 1 and note that 17 of the 36 relate to the Static minus Dynamic (S-D) measures, 8 to a different baseline condition (BGi-RTC BGi), 1 to a resting condition difference (BGi) and the remaining to acceleration/deceleration measures. A similar spread applies to the six and 13 features selected in Methods 1 and 2. The direct association between the features and specific physiology is beyond the scope of this paper. However it is interesting for future researches to investigate a possible association between vestibular stimulation and long-term potentiation in the HC and significantly different resting state observed before a tilt and before returning from a tilt to the beginning position (BGi-RTC BGi). Second, it would be interesting to investigate whether there is a significantly different change in response (S-D) in some pathology due to interplay of excitatory and inhibitory inputs from many sources. Speculatively, it is possible that the selected features are reflections of different waveform shapes and neuronal firing patterns in different brain regions related to vestibular stimulation. The features may be therefore specific to the brain regions and the type of cell firing within a specific brain region. For example, one feature may reflect head direction cell firing in the dorsal HC, whilst another represents place cell firing. A study administering vestibular stimulation by simultaneously acquiring intracranial recordings in various cell types within the three regions known to respond to vestibular stimulation and measuring cell firing from a control region (i.e. one that is not expected to respond to vestibular stimulation) would be a method to investigate this. Another possibility is that each feature represents a specific frequency band of power within each cell firing; this could be investigated by conducting fast Fourier transformations on the data acquired in the study described above and then investigating for phase synchronization between the intracranial recordings and the EVestG signal. For our future studies, we are planning to acquire visuo-spatial performance, MRI and EVestG data at rest and during vestibular stimulation, so that we can further assess the association between EVestG and psychiatric disorders more precisely.

It is likely that EVestG would show even greater diagnostic capability when tested on larger sample size, including a blind study; thereby, building on the current study results. There are a number of directions for future researches, such as investigating whether the central limbic function affects measured signals in the ear, and if so, determining if this is via efferent innervation of the ear or some other routes. Other lines of query could address whether the signals measured in the ear are directly affected by genetic or behavioral manifestations of neuropsychiatric disorders, either directly via altered gene expression or indirectly via humoral or immune influences. We did not examine any probable differences in the EVestG results between patients on and off medication (any of the patient groups who were, or were not, taking medication) because the samples were too small to compare. We also did not control for the type and dosage of medications. Our future efforts would aim to address this in larger samples. The current study builds upon previous research by demonstrating a 4-way separation between clinical psychiatric groups and control subjects using EVestG features. Future studies should use larger samples and utilize multimodal imaging to further explore the neurophysiological underpinnings of EVestG and expand upon the known connections between psychiatric and vestibular symptoms. In addition, multicentre trials and 'blinded' prospective studies are needed to validate the potential of the measured features as surrogate features for psychiatric diagnoses. This diagnostic tool may well assist mental health clinicians to more confidently and accurately diagnose psychiatric illnesses, thereby facilitating earlier treatments and optimally better outcomes.

Acknowledgements

We would like to appreciate Mehrnaz Shoushtarian, Amber Garrett, Ebrahim A. Mousavi, Roger Edwards, Juliana Mitchell-Wong, and Zahra Moussavi for their assistance in study design, data collection and analysis.

Authors' Contributions

All authors significantly contributed to this manuscript.

Financial Disclosure

This study was supported by various grant applications for the clinical trial presented. The Industry Partner, Neural Diagnostics Pty Ltd, who provided the EVestG Facility, has not altered this Paper.

Funding/Support

The study was supported by a grant form the Australian Research Council Industry Linkage to BL and JK, an award from the Australian National Health and Medical Research Council Career Development to JJM, and a grant from the Australian Government Commercialisation Proof-of Concept in association with Neural Diagnostics Pty Ltd.

References

1. Kessler RC, McGonagle KA, Zhao S, Nelson CB, Hughes M, Eshleman S, et al. Lifetime and 12-month prevalence of DSM-III-R psychiatric disorders in the United States. Results from the National Comorbidity Survey. *Arch Gen Psychiatry.* 1994;**51**(1):8–19.

2. Institute of Medicine.. *Evaluation of Biomarkers and Surrogate Endpoints in Chronic Disease*.Washington DC: National Academies Press; 2010.
3. Gurvich C, Maller JJ, Lithgow B, Haghgooie S, Kulkarni J. Vestibular insights into cognition and psychiatry. *Brain Res.* 2013;**1537**:244–59.
4. Balaban CD, Thayer JF. Neurological bases for balance-anxiety links. *J Anxiety Disord.* 2001;**15**(1-2):53–79.
5. Balaban CD. Projections from the parabrachial nucleus to the vestibular nuclei: potential substrates for autonomic and limbic influences on vestibular responses. *Brain Res.* 2004;**996**(1):126–37.
6. Balaban CD. Neural substrates linking balance control and anxiety. *Physiol Behav.* 2002;**77**(4-5):469–75.
7. Schuerger RJ, Balaban CD. Organization of the coeruleo-vestibular pathway in rats, rabbits, and monkeys. *Brain Res Brain Res Rev.* 1999;**30**(2):189–217.
8. Gorman JM, Kent JM, Sullivan GM, Coplan JD. Neuroanatomical hypothesis of panic disorder, revised. *Am J Psychiatry.* 2000;**157**(4):493–505.
9. Muigg P, Hoelzl U, Palfrader K, Neumann I, Wigger A, Landgraf R, et al. Altered brain activation pattern associated with drug-induced attenuation of enhanced depression-like behavior in rats bred for high anxiety. *Biol Psychiatry.* 2007;**61**(6):782–96.
10. Dawson N, Morris BJ, Pratt JA. Subanaesthetic ketamine treatment alters prefrontal cortex connectivity with thalamus and ascending subcortical systems. *Schizophr Bull.* 2013;**39**(2):366–77.
11. Bennett MR. The prefrontal-limbic network in depression: Modulation by hypothalamus, basal ganglia and midbrain. *Prog Neurobiol.* 2011;**93**(4):468–87.
12. Hufner K, Hamilton DA, Kalla R, Stephan T, Glasauer S, Ma J, et al. Spatial memory and hippocampal volume in humans with unilateral vestibular deafferentation. *Hippocampus.* 2007;**17**(6):471–85.
13. Besnard S, Machado ML, Vignaux G, Boulouard M, Coquerel A, Bouet V, et al. Influence of vestibular input on spatial and nonspatial memory and on hippocampal NMDA receptors. *Hippocampus.* 2012;**22**(4):814–26.
14. Cuthbert PC, Gilchrist DP, Hicks SL, MacDougall HG, Curthoys IS. Electrophysiological evidence for vestibular activation of the guinea pig hippocampus. *Neuroreport.* 2000;**11**(7):1443–7.
15. Baek JH, Zheng Y, Darlington CL, Smith PF. Evidence that spatial memory deficits following bilateral vestibular deafferentation in rats are probably permanent. *Neurobiol Learn Mem.* 2010;**94**(3):402–13.
16. Preuss N, Hasler G, Mast FW. Caloric vestibular stimulation modulates affective control and mood. *Brain Stimul.* 2014;**7**(1):133–40.
17. Lithgow B. A methodology for detecting field potentials from the external ear canal: NEER and EVestG. *Ann Biomed Eng.* 2012;**40**(8):1835–50.
18. Heibert D. . Computer models of the vestibular head tilt response, and their relationship to EVestG and Meniere's disease. *Monash Univ.* 2010.
19. Montgomery SA, Asberg M. A new depression scale designed to be sensitive to change. *Br J Psychiatry.* 1979;**134**:382–9.
20. Kay SR, Fiszbein A, Opler LA. The positive and negative syndrome scale (PANSS) for schizophrenia. *Schizophr Bull.* 1987;**13**(2):261–76.
21. Young RC, Biggs JT, Ziegler VE, Meyer DA. A rating scale for mania: reliability, validity and sensitivity. *Br J Psychiatry.* 1978;**133**:429–35.
22. Freund Y,, Schapire RE. *A decision-theoretic generalization of on-line learning and an application to boosting.* 1995. Available from: http://citeseerz.ist.psu.edu/viewdoc/summary?doi=10.http://citeseerz.ist.psu.edu/viewdoc/summary?doi=10.
23. Geisser S. *Predictive Interence*.New York: Chapman and Hall; 1993.
24. A study of cross-validation and bootstrap for accuracy estimation and model selection. *international joint conference on Artificial intelligence.* 1995 Morgan Kaufmann Publishers: pp. 1137–45.
25. Dunn OJ. Multiple comparisons using rank sums. *Technometrics.* 1964;**6**(3):241–52.
26. Cardillo G. *Dunn's test Matlab Central.* 2006. Available from: http://www.mathworks.com/matlabcentral/fileexchange/12827-dunns-tes.
27. Ramirez Basco M, Bostic JQ , Davies D, Rush AJ, Witte B, Hendrickse W, et al. Methods to improve diagnostic accuracy in a community mental health setting. *Am J Psychiatry.* 2000;**157**(10):1599–605.
28. Vitte E, Derosier C, Caritu Y, Berthoz A, Hasboun D, Soulie D. Activation of the hippocampal formation by vestibular stimulation: a functional magnetic resonance imaging study. *Exp Brain Res.* 1996;**112**(3):523–6.
29. Suzuki M, Kitano H, Ito R, Kitanishi T, Yazawa Y, Ogawa T, et al. Cortical and subcortical vestibular response to caloric stimulation detected by functional magnetic resonance imaging. *Brain Res Cogn Brain Res.* 2001;**12**(3):441–9.
30. O'Mara SM, Rolls ET, Berthoz A, Kesner RP. Neurons responding to whole-body motion in the primate hippocampus. *J Neurosci.* 1994;**14**(11 Pt 1):6511–23.
31. Whalley HC, McKirdy J, Romaniuk L, Sussmann J, Johnstone EC, Wan HI, et al. Functional imaging of emotional memory in bipolar disorder and schizophrenia. *Bipolar Disord.* 2009;**11**(8):840–56.
32. Tendolkar I, Weis S, Guddat O, Fernandez G, Brockhaus-Dumke A, Specht K, et al. Evidence for a dysfunctional retrosplenial cortex in patients with schizophrenia: a functional magnetic resonance imaging study with a semantic-perceptual contrast. *Neurosci Lett.* 2004;**369**(1):4–8.
33. Palaniyappan L, Liddle PF. Dissociable morphometric differences of the inferior parietal lobule in schizophrenia. *Eur Arch Psychiatry Clin Neurosci.* 2012;**262**(7):579–87.
34. Maller JJ, Daskalakis ZJ, Thomson RH, Daigle M, Barr MS, Fitzgerald PB. Hippocampal volumetrics in treatment-resistant depression and schizophrenia: the devil's in de-tail. *Hippocampus.* 2012;**22**(1):9–16.
35. Kumar P, Waiter G, Ahearn T, Milders M, Reid I, Steele JD. Abnormal temporal difference reward-learning signals in major depression. *Brain.* 2008;**131**(Pt 8):2084–93.
36. Kuhn S, Gallinat J. Resting-state brain activity in schizophrenia and major depression: a quantitative meta-analysis. *Schizophr Bull.* 2013;**39**(2):358–65.
37. Bluhm RL, Miller J, Lanius RA, Osuch EA, Boksman K, Neufeld RW, et al. Retrosplenial cortex connectivity in schizophrenia. *Psychiatry Res.* 2009;**174**(1):17–23.
38. Bellani M, Ferro A, Brambilla P. The potential role of the parietal lobe in schizophrenia. *Epidemiol Psichiatr Soc.* 2010;**19**(2):118–9.
39. Shepherd AM, Laurens KR, Matheson SL, Carr VJ, Green MJ. Systematic meta-review and quality assessment of the structural brain alterations in schizophrenia. *Neurosci Biobehav Rev.* 2012;**36**(4):1342–56.
40. Brandt T, Schautzer F, Hamilton DA, Bruning R, Markowitsch HJ, Kalla R, et al. Vestibular loss causes hippocampal atrophy and impaired spatial memory in humans. *Brain.* 2005;**128**(Pt 11):2732–41.
41. Stackman RW, Clark AS, Taube JS. Hippocampal spatial representations require vestibular input. *Hippocampus.* 2002;**12**(3):291–303.
42. Sharp PE, Blair HT, Etkin D, Tzanetos DB. Influences of vestibular and visual motion information on the spatial firing patterns of hippocampal place cells. *J Neurosci.* 1995;**15**(1 Pt 1):173–89.
43. Russell NA, Horii A, Smith PF, Darlington CL, Bilkey DK. Long-term effects of permanent vestibular lesions on hippocampal spatial firing. *J Neurosci.* 2003;**23**(16):6490–8.
44. Spiers HJ, Maguire EA. A navigational guidance system in the human brain. *Hippocampus.* 2007;**17**(8):618–26.
45. Maguire EA, Woollett K, Spiers HJ. London taxi drivers and bus drivers: a structural MRI and neuropsychological analysis. *Hippocampus.* 2006;**16**(12):1091–101.
46. Maguire EA, Spiers HJ, Good CD, Hartley T, Frackowiak RS, Burgess N. Navigation expertise and the human hippocampus: a structural brain imaging analysis. *Hippocampus.* 2003;**13**(2):250–9.
47. Ferrari S, Monzani D, Baraldi S, Simoni E, Prati G, Forghieri M, et al. Vertigo "in the pink": The impact of female gender on psychiatric-psychosomatic comorbidity in benign paroxysmal positional vertigo patients. *Psychosomatics.* 2014;**55**(3):280–8.
48. Dudchenko PA, Taube JS. Correlation between head direction cell activity and spatial behavior on a radial arm maze. *Behav Neurosci.* 1997;**111**(1):3–19.
49. Dudchenko PA, Goodridge JP, Taube JS. The effects of lesions of the postsubiculum on hippocampal place cell activity. *Soc Neurosci Abstr.* 1995;**21**:954.
50. Archey WB, Stackman R. W. , Goodridge JP, Dudchenko PA,

Taube JS. Place cells show directionality in an open field following lesions of the head direction cell system. *Soc Neurosci Abstr.* 1997;**23**(504).
51. Maller JJ, Thomson RH, Pannek K, Rose SE, Bailey N, Lewis PM, et al. The (Eigen)value of diffusion tensor imaging to investigate depression after traumatic brain injury. *Hum Brain Mapp.* 2014;**35**(1):227–37.
52. Corcoran KA, Donnan MD, Tronson NC, Guzman YF, Gao C, Jovasevic V, et al. NMDA receptors in retrosplenial cortex are necessary for retrieval of recent and remote context fear memory. *J Neurosci.* 2011;**31**(32):11655–9.
53. Zgraggen E, Boitard M, Roman I, Kanemitsu M, Potter G, Salmon P, et al. Early postnatal migration and development of layer II pyramidal neurons in the rodent cingulate/retrosplenial cortex. *Cereb Cortex.* 2012;**22**(1):144–57.
54. Baiano M, David A, Versace A, Churchill R, Balestrieri M, Brambilla P. Anterior cingulate volumes in schizophrenia: a systematic review and a meta-analysis of MRI studies. *Schizophr Res.* 2007;**93**(1-3):1–12.
55. Allen P, Laroi F, McGuire PK, Aleman A. The hallucinating brain: a review of structural and functional neuroimaging studies of hallucinations. *Neurosci Biobehav Rev.* 2008;**32**(1):175–91.